Journal of Power Sources, 40 (1992) 271–282

Electrical breakdown phenomena in $(PEO)_xLiF_3CSO_3$ ion-conducting polymers

C. A. C. Sequeira* and A. Hooper
The Harwell Laboratory, Didcot, Oxon. OX11 ORA (UK)

(Received March 4, 1990; in revised form June 9, 1992)

Abstract

Electrical breakdown of $(PEO)_xLiF_3CSO_3$ polymers (with $x=4$ to 14) has been studied using lithium electrode systems, in the temperature range 100–170 °C. The observed breakdown characteristics depend particularly on the temperature, the thickness of the polymer sample and the mechanical load applied to the cell stack. Breakdown is localized and it is likely that its source lies in poor contact between the electrodes and the polymer (and possibly inhomogeneities in the latter) leading to 'hot spots' where the current density is high enough to induce decomposition.

Introduction

The phenomenon of cell failure in polymer–electrolyte-based lithium batteries is of great commercial importance [1–3]. Although the study and use of ionically-conducting polymers is well reported in the open literature [4–10], little is known about electrical breakdown phenomena which might occur in such materials. This report describes observations of breakdown in poly(ethylene oxide) $(PEO)_xLiF_3CSO_3$ polymers under d.c. bias conditions. Such a process in the electrolyte of an electrochemical cell may lead to device failure and is therefore worthy of detailed analysis.

Experimental

Sample discs, ≈ 30 μm thick, were cut from polymer–electrolyte films of varying composition, within the $(PEO)_xLiF_3CSO_3$ ($x=4$ to 14) system, prepared by a 'doctor blade'-casting technique. The discs were mounted either singly or in layers between lithium foil electrodes in one of two types of cell case. The first, originally designed to measure cell dimension changes, was mounted within a closed furnace tube (TO 50 Büchi tube) under flowing argon gas and a light applied mechanical loading. The second was free standing within an argon flushed dry box (<5 ppm H_2O) and allowed for the application of higher and variable loadings.

In some cases, a third, pseudo-reference, electrode comprising a 0.03 mm diameter nickel wire was positioned between appropriate layers of the electrolyte.

*Present address: Instituto Superior Técnico, Technical University of Lisbon, Avenue Rovisco Pais, 1096 Lisboa Cedex, Portugal.

0378-7753/92/$5.00

Discharge current (d.c.) voltages were applied via a ramp generator and potentiostat (Thomson) and subsequent current and voltage behaviour monitored using Keithley electrometers with output to x–y and x–t recorders. Complimentary a.c. measurements were made using a Solartron 1174 Frequency Response Analyser. The physical nature of samples which exhibited electrical breakdown characteristics was studied using scanning electron or optical microscopy. In the latter case, the microscope was mounted with direct viewing into the dry box system.

Results

Current-voltage measurements

One manifestation of electrical breakdown in the $(PEO)_xLiF_3CSO_3$ electrolyte is observed on application of a linear ramp voltage to a cell employing two lithium foil electrodes, when, at some point, sudden pulses of current are observed above the normal cell current. The first of these pulses indicates the initiation of breakdown, which can then be defined by the corresponding breakdown current (I_B), the important variable, or the parameter that follows it, the breakdown voltage (V_B). Table 1 contains

TABLE 1

Breakdown data on $(PEO)_x/LiF_3CSO_3$ polymers from polarized Li/Li cells

$(PEO)_x/LiF_3CSO_3$ concentration (x)	Temperature (°C)	Breakdown voltage, V_B (mV)[a]	Breakdown current, I_B (mA)[a]	Breakdown charge, Q_B (C)[b]
4	100	315	0.48	0.97
	120	75	0.93	0.65
	140	24	2.02	3.67
	160	18	3.89	8.40
6.5	100	1700	0.25	1.38
	120	1600	0.35	2.44
	140	630	1.05	4.06
	160	40	5.25	14.33
9	100	147	1.20	1.49
	120	86	1.48	1.85
	140	36	1.91	1.80
	160	21	3.71	8.17
	170	15	5.80	18.76
11.5	100	630	0.62	2.07
	120	82	1.63	2.28
	140	24	2.70	4.13
	160	17	4.30	9.61
14	100	86	1.02	0.90
	120	54	1.94	2.39
	140	20	3.20	5.43
	160	25	6.70	23.32

[a]Potentiodynamically-polarized cells.
[b]Galvanostatically-controlled cells.
Area = 4.9 cm^2. Thickness = 120 μm. Ramp speed = 6 mV min^{-1}.

data obtained for a number of polymer compositions and temperatures with a total electrolyte thickness of 120 μm (4 layers) and ≈ 5.0 cm^2 area. The ramp speed was 6 mV min^{-1}. In all cases there is a trend towards higher breakdown voltages at lower temperatures. This trend suggests a relationship between the electrical breakdown and the mechanical properties of the polymer. However, the observed trend could equally be due to the fact that the electrolyte resistance increases as temperature is decreased leading to a greater proportion of the applied voltage being dropped across the bulk electrolyte, so that the potential drop at the electrodes is less. With the exception of the $x=6.5$ sample, the compositional and temperature variation of the breakdown voltage is small in the range 120 to 160 °C for $x=4$ to 14.

A similar relationship is obtained for the temperature dependence of I_B: this time there is a trend towards lower breakdown currents at lower temperatures. It should be noted that repeated experiments lead to V_B values more reproducible than the I_B values (10% deviation for V_B as compared to $\approx 20\%$ for I_B). This lack of reproducibility may be related to the difficulty of defining precise 'true' electrode areas.

Experiments performed at several supply voltage sweep rates lead to identical patterns. However, higher V_B, I_B values are measured at higher voltage sweep rates.

The influence of electrode spacing on the breakdown initiation has also been studied for a number of electrolyte thicknesses (4–32 layers). In all cases there is a marked effect of the electrode spacing on V_B; for example, cell voltages as high as 0.8 V or 2.5 V can be applied across a Li/Li cell held at 120 °C when using 0.36 mm or 0.96 mm $(PEO)_9LiF_3CSO_3$ samples, respectively, without breakdown observation.

One aspect, particularly relevant to battery cycling, is related to observations made on the effect of polarization reversal on the electrical breakdown phenomenon. This is illustrated in Fig. 1. If the voltage sweep is reversed immediately after initiation of breakdown, a subsequent polarization decline to zero cell voltage occurs without any current pulse. A new progressive polarization leads to a V_B value that practically does not differ from the previous one. Successive polarizations in a progressive-regressive mode did not differ too much from the first cycling. Visual and microscopic investigation of the sample showed a slight degree of damage consisting of many minute darkened or black particles distributed in an apparently random fashion (Fig. 2). It is clear therefore, that breakdown initiates at very localized areas in the polymer film; its initial stage seeming to be relatively slow. But, if the voltage rate is reversed after the occurrence of intense breakdown, it is not possible to avoid its propagation in the preceding polarization run down to zero cell voltage (Fig. 1). Successive polarization cycles lead to intense damage. The darkened spots within the polymer, characteristic of the breakdown initiation stage, change, through black char-like regions, to the formation of actual holes through the membrane which can be up to 1 mm in diameter (Fig. 3). The damage propagates across the entire polymer membrane as cycling under breakdown conditions is prolonged.

Voltage–time measurements

The quantities V_B and I_B are not invariant with operating parameters such as the rate of the applied voltage ramp and therefore do not represent absolute threshold levels. A quantity which correlates more directly with the onset of breakdown is the amount of charge, Q_B, which has passed through the cell. Accurate Q_B measurements were obtained by a galvanostatic technique. The time at which a sudden decrease was observed enabled the definition of the breakdown initiation. As illustrated in Fig. 4 for a 120 μm thick electrolyte, the first voltage pulses have small amplitude occurring

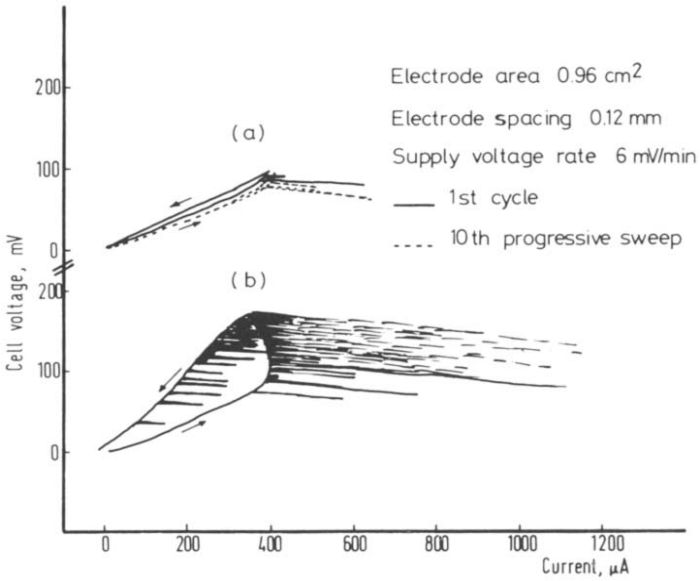

Fig. 1. Potentiodynamic behaviour of a Li|$(PEO)_9LiF_3CSO_3$|Li cell at 120 °C. Regressive sweep initiated (a) immediately after breakdown initiation, and (b) after intensive breakdown has occurred.

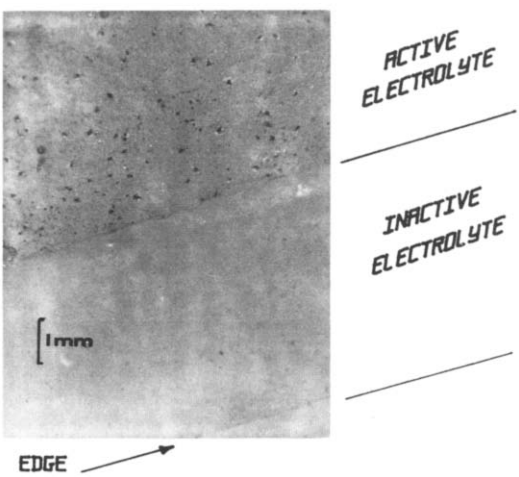

Fig. 2. Electrical breakdown damage in a film of $(PEO)_9LiF_3CSO_3$ polymer–electrolyte.

at different time intervals. But once the propagation process is initiated, continuous and larger peaks occur leading to intense cell damage.

The magnitude of Q_B increases significantly with the mechanical load which is applied to the cells and this may be simply related to the improvement in electrode/electrolyte contact and corresponding increase in effective cell area as the load is applied. This effect is also apparent from measurements of cell resistance using a.c.

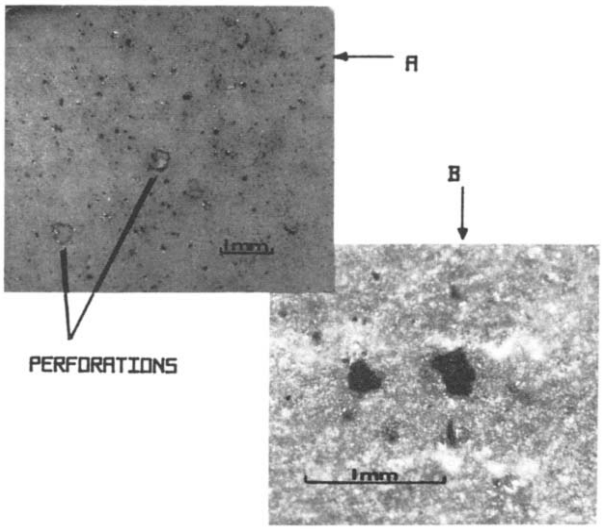

Fig. 3. Typical electrical breakdown damage in a $(PEO)_9LiF_3CSO_3$ polymer–electrolyte film of 35 μm thickness: (a) perforations through film, (b) black carbonized regions.

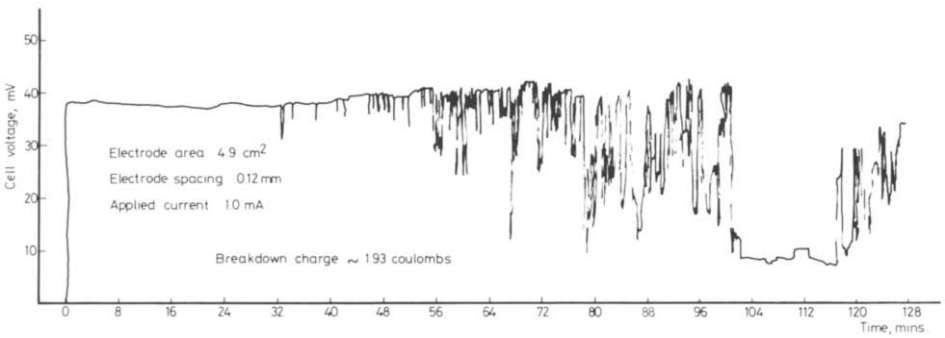

Fig. 4. Galvanostatic behaviour of a Li|$(PEO)_9LiF_3CSO_3$|Li cell at 120 °C.

impedance techniques (see below). At a particular cell loading, Q_B is relatively insensitive to both the composition of the electrolyte $(PEO)_xLiF_3CSO_3$ for $4 \leqslant x \leqslant 14$ and the preparation of the lithium electrode surface, either as-received or polished. It is, however, a strong function of both temperature and electrolyte thickness, being higher for greater thicknesses (Table 2) and higher temperatures.

Postmortem analyses of the cell components submitted to Q_B measurements for different temperatures, electrode spacings and electrolyte concentrations, showed that the lithium-exposed areas remain bright and grey metallic as before the experiments, but minute black spots were found, sometimes, at the anode surface. Lumps of black material were always found in the polymer discs, which sometimes also showed nonuniformly distributed dark brown areas. Observation of a thicker polymer sample showed a triangular pattern, but this could not be followed by peeling off the external polymer layers. Although the internal layers also contained black spots, it was realized

TABLE 2

Influence of electrode spacing on Q_B at constant temperature (120 °C), for $(PEO)_9LiF_3CSO_3$ samples

Spacing (mm)	Q_B (C/cm^2)
0.12	0.4
0.36	3.5
0.96	112

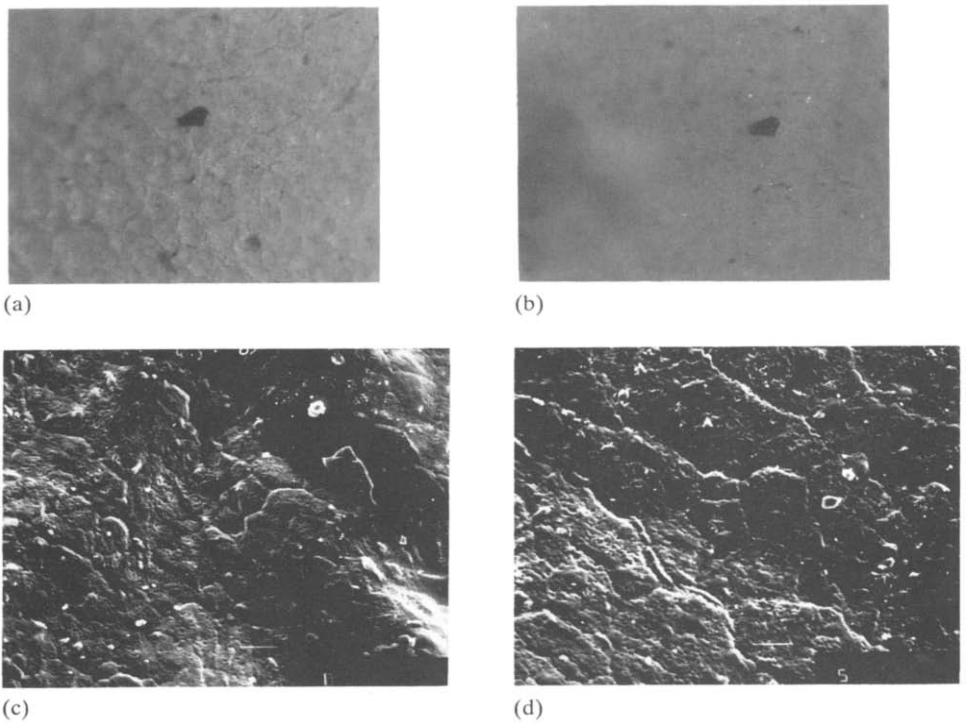

Fig. 5. (a, b) Triangular pattern and (c, d) external aspect of a $(PEO)_9LiF_3CSO_3$ thick sample after breakdown at 120 °C (magnification 200×).

that gross damage occurred mainly at the external polymer layers. Figure 5 illustrates these observations.

Complementary a.c. analysis

Following the systematic d.c. studies described above, combined d.c. and a.c. techniques, which have found increasing interest in the elucidation of electrochemical processes involved in many battery and energy sources [11, 12] were employed. In general, the a.c. impedance measurements were performed in a 100 kHz to 1 Hz range, before and after polarizing Li/Li cells by one of the d.c. methods described

above. Then, the results of the impedance plots were correlated with the results of the polarization measurements, so enhancing our understanding of the damage phenomenon.

Proceeding this way, it was possible to estimate the effect of some variables on the electrical breakdown, as reported below:

(i) The value of the breakdown charge measured on nonpolished lithium electrodes, immediately after assembly, was smaller than the corresponding value measured on polished lithium electrodes; but, the values are identical if measurements are performed 5 to 24 h after equilibration. This result is in agreement with low-frequency measurements of the Li/Li cell resistance, as shown in Fig. 6. It may be concluded that the effect of an oxide film at the lithium surface does not affect the breakdown characteristics, particularly if measurements are performed $\geqslant 5$ h of keeping the cell at the working temperature.

(ii) The effect of applied pressure to the cell stack seems to play an important role, concerning the breakdown phenomenon. In fact, it has been observed that the breakdown charge increases strongly with increasing applied pressure to the cell, its value for a particular pressure being independent of the lithium surface state. Once more, this finding agrees with the low-frequency resistance trend obtained under strong load conditions, as shown in Fig. 6. Therefore, the threshold levels reported above should be regarded as 'minimum breakdown charges', being clear that the higher the mechanical load applied to the cell stack the higher the $Li/(PEO)_xLiF_3CSO_3$ contact interface, which suggests that the critical breakdown factor is actually the charge/unit effective area (Q_B/cm^2).

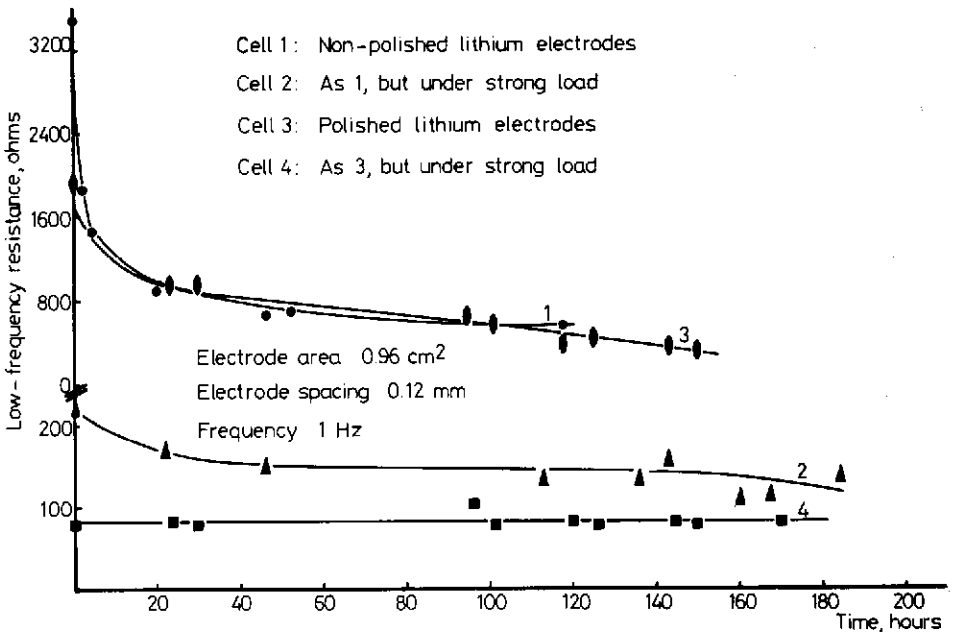

Fig. 6. $Li|(PEO)_9LiF_3CSO_3|Li$ low-frequency cell resistance against time at 120 °C, for different experimental conditions.

(iii) The effect of preheating at 140 °C, before the breakdown tests are performed, was seen to have no effect on the damage. In this respect, a Li/Li cell was kept at 140 °C for about 100 h. Then, its temperature was lowered to 120 °C and an impedance plot was obtained, as shown in Fig. 7(a). Subsequently, the cell was potentiostatically polarized at ≈200 mV for about 3 h. As a result, gross damage was initiated after about 30 min of cell polarization. The shape of the peaks observed for a 3-minute interval was followed carefully by I/t measurements. Most of the peaks had a square shape, but very erratic behaviour was observed as breakdown propagation continued. Once the applied electric field was disconnected, a new a.c. plot was taken. This is shown in Fig. 7(b). A repeated procedure with a non-preheated cell led to very similar results.

Analysis of Fig. 7 shows that apart from partial destruction of the capacitive semicircle, the main effect of breakdown is related with the low- and high-frequency resistance values. Before polarization, these values were about 780 and 650 Ω, and after damage occurrence they were about 325 and 650 Ω, respectively. The high-frequency limit of the impedance is generally equal to the electrolyte resistance. Therefore, the fall in cell resistance ($780 - 325 = 455\ \Omega$) can be ascribed almost completely to the polymer-resistance decrease ($650 - 200 = 450\ \Omega$). This strongly indicates that the breakdown occurs inside the polymer–electrolyte itself, as further confirmed by visual and optical microscopic observation of the polymer samples which showed many darkened or black (carbonized) regions, and even holes. In comparison, the lithium surfaces were always bright and showed no signs of damage.

Three-electrode cell measurements

The studies reported above led to the idea that the breakdown phenomena are directly connected with a process which involves ionic conductivity and electrochemical charge transfer reactions.

To further demonstrate this mechanism, a nickel pseudo-reference electrode was employed. The potential of this nonreversible nickel wire was shown to be reproducible, stable and unpolarizable in the polymer–electrolyte. Therefore, the nickel electrode was used with confidence as reference for the present purposes. The results of d.c. tests carried out with Li/Li cells including a nickel electrode were as follows:

(i) I/V measurements, immediately after V_B, slight potential variations were observed at both lithium electrodes, whose duration was of the same order of the duration of the current pulses.

(ii) V/t measurements, under galvanostatic conditions, sudden decreases in cell voltage were accompanied by corresponding potential variations at the lithium electrodes.

(iii) I/t measurements, under potentiostatic conditions, sudden increases in circuit were accompanied by an anode potential variation larger than that found at the cathode. These electrode potential variations remained for short times once the current pulses had occurred. Current enhancement and subsequent F_3CSO_3-anion discharge may be the reason for the larger anode overpotential observed.

A second set of tests was carried out in which one lithium electrode was polarized, instead of the whole cell. I/E, E/t and I/t measurements were conducted in both directions (the working lithium electrode acting as anode and as cathode) and did not enable us to attribute the breakdown phenomenon to a particular electrode site. This is in agreement with previous findings.

In summary, the breakdown phenomena reported here do not occur either at the negative or at the positive electrode interface, as found in many materials [13–16], but within the polymer itself, as a consequence of charge transfer.

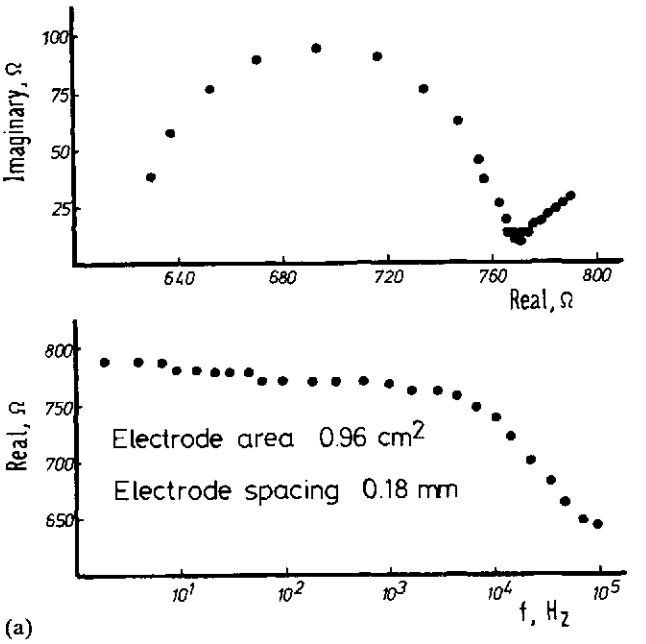

(a)

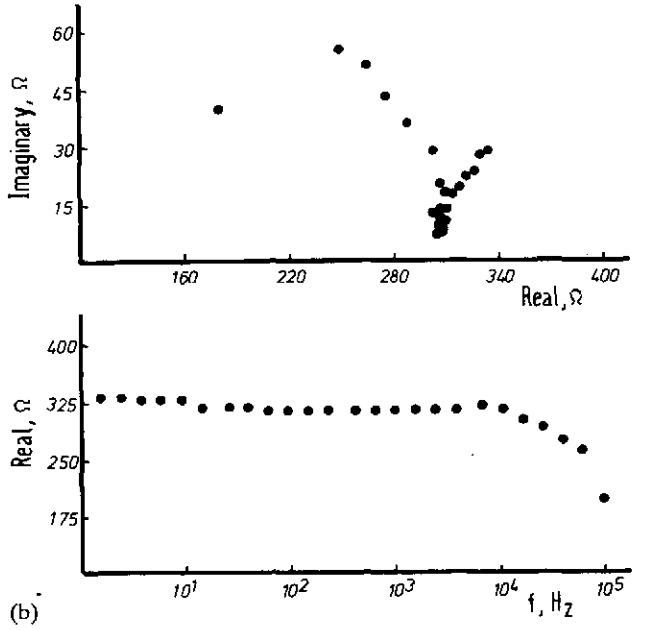

(b)

Fig. 7. The a.c. impedance spectra for a Li|$(PEO)_9LiF_3CSO_3$|Li cell at 120 °C, over the frequency range 100 kHz to 1 Hz, 5 points per decade: (a) before cell polarization, (b) after intense breakdown occurrence by polarizing the cell at 200 mV for 3 h.

Discussion and conclusions

Lithium solid-state cells offer both high energy densities and long shelf lives. An additional important criterion for any cell is its operating lifetime. Consequently, it is important to identify and characterise failure mechanisms which may occur within the cell during operation.

During the galvanostatic cycling of solid-state cells comprising a lithium metal anode, a polymeric $(PEO)_9LiF_3CSO_3$–electrolyte and a composite, V_6O_{13}/polymer–electrolyte/carbon cathode, a failure mode involving the degradation of the electrolyte membrane has been observed (Fig. 8). The phenomenon is manifested by the superposition of sharp, intermittent voltage excursions on the normal cell *emf*-capacity curves. It occurs both on the charge and discharge cycles of the cell and is towards higher voltages on charge and lower values on discharge. Observation of the effect has been confined to cells constructed by the wrapping of sheet cell components into a cylindrical 'Swiss-roll, configuration with an effective area of 200 cm^2. In such cells it has occurred at nominal current densities below 0.1 mA cm^{-2} at temperatures in the range of 120 to 140 °C. Both smaller (1 cm^2) cells of a simple sandwich design and cells of a comparable area (100 cm^2), but of a folded construction, have been cycled for long periods (i.e., upwards of 100 cycles), giving good performance. In both of these types of cell, the active assembly is placed under a positive mechanical loading. In the cylindrical configuration the amplitude of the voltage excursions and the subsequent damage to the electrolyte membrane was reduced by a tighter winding of the cell. Changes in the physical appearance of the electrolyte are of a localised nature and range from the appearance of carbon spots to the formation of real perforations through the membrane (Fig. 9); in other words, the physical nature of the electrolyte after damage is similar to that described in the previous section, for Li/Li cells.

In order to characterize more fully and to gain a better understanding of the mechanisms involved in the observed breakdown phenomenon in real cells, a number of polymer compositions have been studied. Current-voltage, galvanostatic, potentiostatic and a.c. impedance experiments have been carried out using Li/Li electrode cells

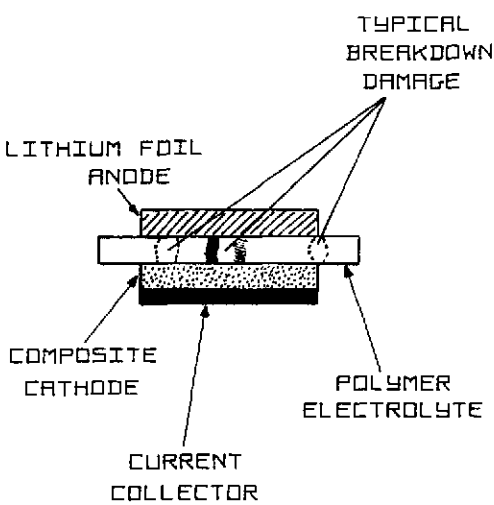

Fig. 8. Schematic of voltage-breakdown damage.

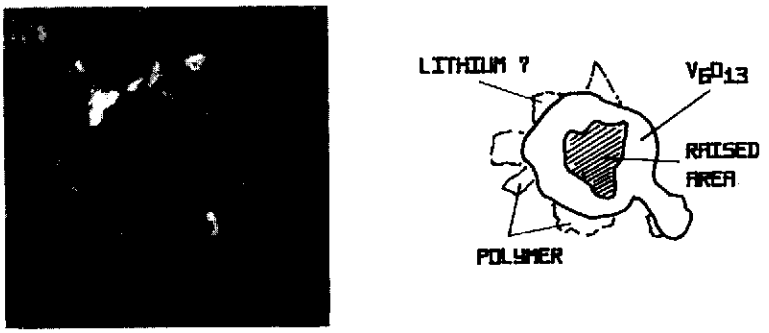

Fig. 9. Detail of a breakdown-related perforation in a 35 μm $(PEO)_9LiF_3CSO_3$ polymer–electrolyte film supported on a V_6O_{13}-based cathode.

(100–170 °C). Visual and optical techniques have also been employed. The results, although there were some experimental uncertainties, are in broad agreement, showing that the onset of breakdown is associated with the passage of a critical charge density in the polymer. The value of this critical charge density relates to the passage of charge in one direction only. In other words, breakdown can be suppressed by charge reversal. This last characteristic is, of course, most significant in relation to real cell operation and shows that the total amount of charge passed and hence, cell lifetime at a given current drain can be largely provided that Q_B is not exceeded on any single half-cycle.

Observance of the above criterion together with the use of configurations which ensure good interfacial contacts (e.g. appropriate external load, elimination of possible interfacial resistance) has produced cells with long cycle lives.

At 120–140 °C, lives in excess of 150 deep discharge cycles, with total charge passage in excess of 1000 C cm^{-2}, have been obtained, for LiV_6O_{13} cells [3].

The presence of high-current densities in other solid electrolyte cells has been associated with the formation of metallic dendrites. Such a model would not be inconsistent with the visual observations of the $(PEO)_xLiF_3CSO_3$ polymer after breakdown. However, the graphical form of the breakdown effect observed on the LiV_6O_{13} cells suggests that it is not due to the formation of lithium dendrites through the electrolyte membrane. In fact, dendrite formation would not normally be expected to occur on discharge and would always lead to electronic shorting. In fact, the detail of the voltage transients under galvanostatic conditions for both types of cell indicates a relatively slow increase of the cell resistance followed by a sharp return to the normal operating conditions. Initially, a few random transients are observed followed by an avalanche of breakdown effects. In some cases, even after prolonged breakdown, relatively quiet periods are observed in both the high- and low-resistance states. One possible explanation of this increasing cell resistance is the formation of depletion regions within the electrolyte at the cathode interface which may occur as a result of the presence of anionic as well as cationic transport [17], which is known to exist in these materials [1]. Of course, the presence of anionic transport in the polymer will lead to compositional variations, which induce high resistance regions. These electrolyte inhomogeneities are accompanied by the generation of high electrical current densities, which are enough to induce physical damage (heating, decomposition) of the electrolyte. In this respect, it should be noted that the thermal stability of PEO is known to be low at the temperatures of the present experiments even in the absence

of an applied potential. Breakdown via this mechanism will obviously be limited to regions where ionic currents are originally flowing and will hence be related to the quality of the electrolyte/electrode interfaces. Poor interfacial contact and a nonuniform initial current distribution will lead to islands of high resistance, or 'hot spots', which are active sites for the observed local degradation. The formation of any other high-resistance layer within the cell (e.g., insulating films via reaction of lithium with water) would also be susceptible to breakdown of this type. In this context, it is well known that such layers (as seen in Fig. 7) may significantly affect the current and that their resistance values are time dependent when d.c. is passed.

The electrochemical model is consistent with the observation that breakdown can be suppressed by charge passage reversal and would also predict an increase in the value of the critical charge density with increasing electrolyte thickness (longer time to establish compositional changes) and temperature (compositional variation limited by diffusion effects).

The results of this work, we believe, are valid and of interest to the operation of complete polymer–electrolyte cells. However, the analysis of the data is difficult since there are many possibilities, and, other interpretations, as equally appropriate as those presented here, are open for consideration.

References

1 J. M. North, C. A. C. Sequeira, A. Hooper and B. C. Tofield, *Ext. Abstr., 1st Int. Meet. Lithium Batteries, Rome, Apr. 1982,* Abstr. No 32.
2 C. A. C. Sequeira and A. Hooper, *Ext. Abstr., Electrochemical Society, Spring Meet., San Francisco, CA, May 1983,* Abstr. No 493.
3 A. Hooper and J. M. North, *Solid State Ionics, 9/10* (1983) 1161–1166.
4 R. Dupon, D. H. Whitmore and D. F. Schriver, *J. Electrochem. Soc., 128* (1981) 715–717.
5 M. Armand, J. M. Chabagno and M. J. Duclot, *Ext. Abstr., 2nd Int. Conf. Solid Electrolytes, St. Andrews, Scotland, Sept. 20–22, 1978,* Abstr. 6.5.
6 B. Scrosati (ed.), *2nd Int. Symp. Polymer Electrolytes,* Elsevier Applied Science, Barking, UK, 1990.
7 M. A. G. Martins and C. A. C. Sequeira, *J. Power Sources, 32* (1990) 107–124.
8 M. J. C. Plancha, C. M. Rangel and C. A. C. Sequeira, *Ext. Abstr., Electrochemical Society, Spring Meet., Washington, DC, May 1991.*
9 J. S. Lundsgaard and R. Koksbang, in C. A. C. Sequeira (ed.), *Chemistry and Energy – I,* Elsevier Amsterdam/New York, 1991, pp. 153–162.
10 C. A. C. Sequeira, A. Hooper and J. M. North, *Solid State Ionics, 13* (1984) 175–179.
11 A. Hooper, *J. Electroanal. Chem., 109* (1980) 161–166.
12 A. Hooper, *Solid State Ionics, 5* (1981) 399–402.
13 R. D. Armstrong, T. Dickinson and J. Turner, *Electrochim. Acta, 19* (1974) 187–191.
14 D. S. Demott and B. A. W. Redfern, *J. Phys., 37* (1976) C7–423.
15 R. H. Richman and G. J. Tennenhouse, *J. Am. Ceram. Soc., 58* (1975) 63–67.
16 A. Hooper, *Trans. J. Ceram. Soc., 79* (1980) 134–138.
17 S. Atlung, K. West and T. Jacobsen, in D. W. Murphy, J. Broadhead and B. C. H. Steele (eds.), *Materials for Advanced Batteries,* NATO Conference Series, Plenum, New York/London, 1980.